PCCP

Physical Chemistry Chemical Physics

www.rsc.org/pccp

Volume 11 | Number 15 | 21 April 2009 | Pages 2561–2780

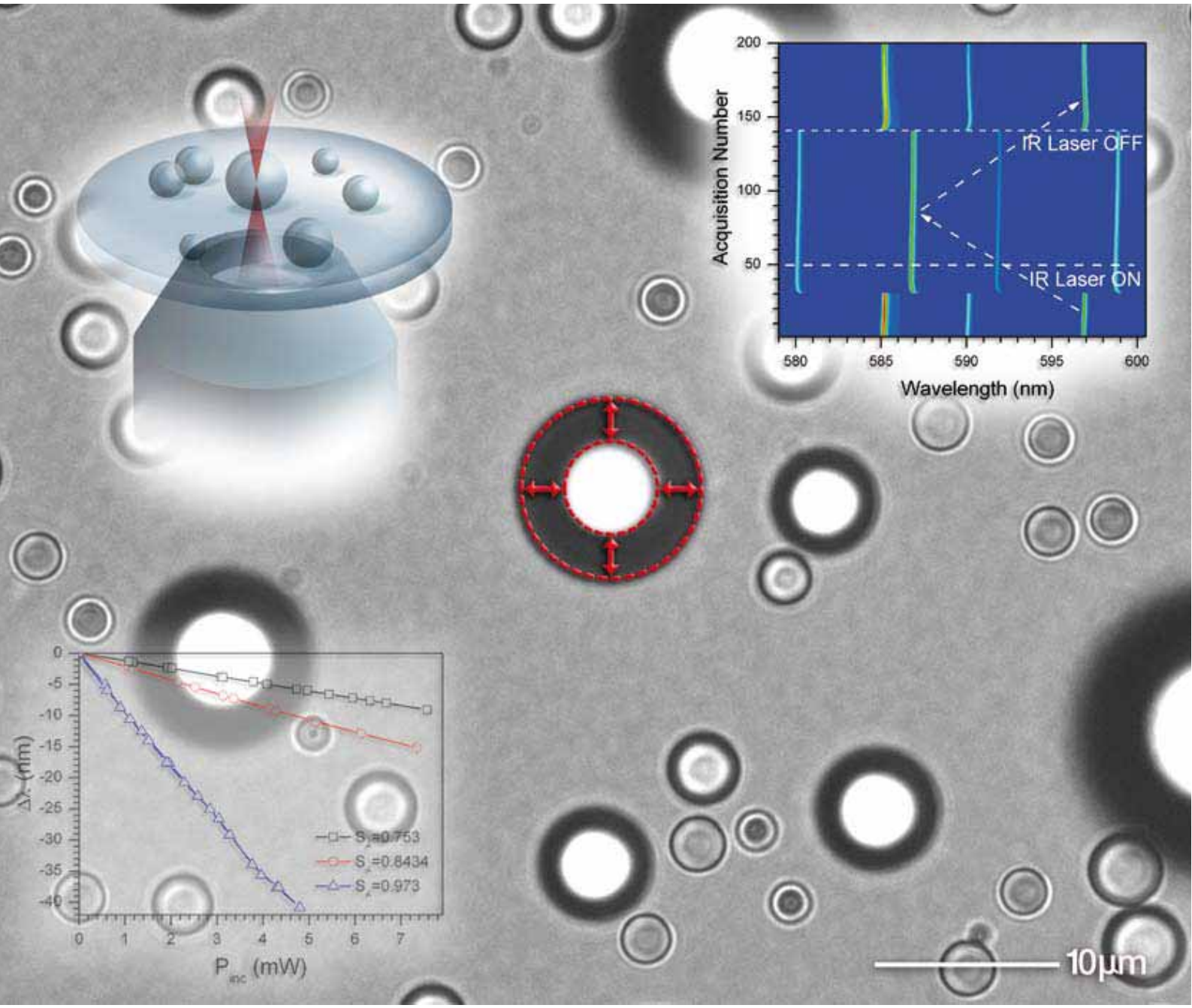

ISSN 1463-9076

Reversible photothermal tuning of a salty water microdroplet

A. Kiraz,*[a] Y. Karadag,[a] S. C. Yorulmaz[a] and M. Muradoglu[b]

Received 24th September 2008, Accepted 29th January 2009
First published as an Advance Article on the web 12th February 2009
DOI: 10.1039/b816784b

A fully reversible photothermal tuning of an inorganic salt (NaCl)–water microdroplet standing on a superhydrophobic surface is demonstrated. The size change of the microdroplet is caused by a focused infrared laser beam in a humidity-controlled chamber and a fully reversible large spectral tuning up to ~40 nm is achieved. The evaporation and growth of the microdroplet are modeled using a lumped system formulation of mass and energy conservations and a good agreement is observed between the experimental and theoretical results.

The evaporation and growth of salty water droplets have been extensively studied mainly in the context of aerosol science.[1] It is well known that vapor pressure decreases at the surface of a salty water droplet with the amount of salt in the solution. Consequently, a salty microdroplet (aerosol) reaches an equilibrium size in an atmosphere that is not saturated with water vapor. Under local heating, such an aerosol that is initially at equilibrium with the surrounding atmosphere will shrink to a new equilibrium size with a higher salt concentration. Upon the removal of local heating, the size of the aerosol will increase, and the aerosol will completely recover its original size. Hence local heating is an ideal tool to reversibly change the size of an aerosol of an aqueous salt solution.

In this letter we demonstrate fully reversible spectral tuning of the whispering gallery modes (WGMs) of salty water microdroplets standing on a superhydrophobic surface through reversible size changes caused by local heating with a focused infrared laser. Such a large, reversible spectral tuning of an optical microcavity[2] can be important for applications in short-haul optical communication systems[3] that use visible light sources and plastic fibers, and in water-based opto-fluidics systems.[4] The technique we present can also be used in fundamental studies in aerosol chemistry.[1]

The present work is motivated by our recent study on the spectral tuning in glycerol–water microdroplets standing on a superhydrophobic surface through local heating with a focused infrared laser.[5] It has been shown that even the slight volatility of glycerol may result in significant irreversibility especially in small relative humidity conditions and thus a full reversibility requires replacement of the less volatile component (glycerol) with an ideally nonvolatile substance. An inorganic salt such as NaCl used here thus appears to be an ideal alternative since it is ideally nonvolatile and highly soluble in water.

[a] *Department of Physics, Koç University, Rumelifeneri Yolu, 34450 Sariyer, Istanbul, Turkey. E-mail: akiraz@ku.edu.tr*
[b] *Department of Mechanical Engineering, Koç University, Rumelifeneri Yolu, 34450 Sariyer, Istanbul, Turkey*

Photothermal modulation of the WGMs was previously used to study the absorption spectrum of single suspended aerosols.[6–9] These demonstrations relied on measuring the modulation of the Mie scattered light intensity in response to a modulated infrared light source. This technique did not require large spectral tuning of individual WGMs, hence reported spectral tuning ranges were limited to ~1 nm at around 590 nm. In this study we demonstrate that spectral tuning by up to ~40 nm can be achieved by salty water microdroplet systems.

Following Tu and Rai[10] and Kiraz *et al.*,[5] the evaporation and growth of a salty water microdroplet that is locally heated with a focused infrared laser are modeled using the lumped system formulation of mass and energy conservations. The derivation and details of the model equations can be found in ref. 5 and 10. Nevertheless the model is briefly described here for completeness. According to this simple model, the number of moles N_A of component A (water) in the microdroplet of radius a and the temperature T of the microdroplet evolve by

$$\frac{dN_A}{dt} = -4\pi a f_{PB} D_A \frac{P_A^0(T_\infty)}{RT_\infty}(\gamma_A x_A \phi_A - S_A), \quad (1)$$

$$\frac{dT_d}{dt} = \frac{\Delta H_{vap,A}}{NC_{PL}}\frac{dN_A}{dt} - \frac{3k_{eff}V_m}{a^2 C_{PL}}(T_d - T_\infty) + \frac{\tilde{Q}_{abs}P_{inc}}{NC_{PL}}, \quad (2)$$

where

$$\phi_A = \left(\frac{T_\infty}{T_d}\right)\frac{P_A^0(T_d)}{P_A^0(T_\infty)}. \quad (3)$$

In eqn (1)–(3), D_A, γ_A, x_A, S_A, R, $P_A^0(T)$, V_m, N, C_{PL}, $\Delta H_{vap,A}$, and k_{eff} represent the molecular diffusivity in the gas mixture, the activity coefficient, the mole fraction, the relative water humidity in the chamber, the universal gas constant, the vapor pressure at temperature T, the molar specific volume, the total number of moles, molar heat capacity of the microdroplet mixture, the enthalpy of evaporation, and the effective heat conductivity, respectively. T_d and T_∞ are the temperatures at the microdroplet interface and in the chamber far from the microdroplet, respectively. The correction factor f_{PB} is introduced in eqn (1) in order to account for the effects of the substrate on the mass transfer and is specified by Picknett and Bexon[5,11,12] equation. Based on the experimental results obtained for millimetre-size NaCl–water droplets standing on the superhydrophobic surface used in the experiments, the contact angle is taken between θ = 150–160°, which yields correction factors of f_{PB} = 0.6727–0.6840. For NaCl, the water activity coefficient (γ_A) and solution density (ρ)

in g cm^{-3} are calculated using the polynomial best fits given by ref. 13 as

$$\gamma_A = \sum_{i=0}^{i=4} C_i x_{WP}^i;\ \rho = \sum_{i=0}^{i=4} A_i x_{WP}^i, \qquad (4)$$

where $C_0 = 1.0$, $C_1 = -6.366 \times 10^{-3}$, $C_2 = 8.624 \times 10^{-5}$, $C_3 = -1.158 \times 10^{-5}$, $C_4 = 1.518 \times 10^{-7}$, $A_0 = 0.9971$, $A_1 = 7.41 \times 10^{-3}$, $A_2 = -3.741 \times 10^{-5}$, $A_3 = 2.252 \times 10^{-6}$, $A_4 = -2.06 \times 10^{-8}$, and x_{WP} represents the solute weight percent. Following Kiraz *et al.*,[5] k_{eff} is calculated as the area average of the heat conductivities of the air (k_a) and the substrate (k_s), *i.e.* $k_{eff} = f_a k_a A_a + (1 - f_a)k_s$ where $f_a = A_a/A_d$ is the ratio of the surface area of the microdroplet that is in contact with the air and the total surface area of the microdroplet. Modified absorption efficiency ($\tilde{Q}_{abs}$) is the ratio of the total power absorbed by the microdroplet to the total power of the incident beam (P_{inc}). Generalized Lorenz–Mie theory[14–16] is used to calculate $\tilde{Q}_{abs}$ for a laser beam focused to the microdroplet's center, assuming a focal waist (focal radius) of $w_0 = 1000$ nm. In the calculations, the real part of the refractive index of water is taken as 1.33, independent of the amount of NaCl dissolved in the microdroplet. The imaginary part of the refractive index is calculated using a linear relationship between NaCl concentration and the water absorption coefficient.[17,18]

Superhydrophobic surface preparation, microdroplet generation, and the optical setup were reported previously.[5] The experimental setup is also sketched in Fig. 1a. Superhyrophobic surfaces are prepared by spin coating 20–50 mg ml^{-1} ethanol dispersions of hydrophobically coated silica nanoparticles (Evonik, Aeroxide® LE1, LE2). NaCl–water microdroplets are sprayed on to the superhydrophobic surface using an ultrasonic nebulizer from a 1.7 M NaCl–water solution containing 20 μM Rhodamine B while glycerol–water microdroplets are generated from a 90 : 10 volume distribution of glycerol–water solution containing 5 μM Rhodamine B. Upon generation of the microdroplets, the superhydrophobic surface containing the microdroplets is placed in a humidity chamber whose relative humidity is kept constant at 0.753, 0.8434, or 0.973 by saturated water solutions of NaCl, KCl, or K_2SO_4, respectively as shown in Fig. 1a. Optical experiments are performed after waiting for at least 2–3 h to allow the microdroplets to reach their equilibrium sizes in the humidity chamber. A cw solid-state green laser ($\lambda = 532$ nm) and a cw solid-state infrared laser ($\lambda = 1064$ nm) are used for exciting the Rhodamine B molecules and for local heating, respectively. The beams of both lasers are combined with a beam splitter, reflected off a dichroic mirror, and focused with a high numerical aperture microscope objective (NA = 1.4, 60×) in the inverted geometry. The green and infrared lasers are focused to the rim and center of individual microdroplets, respectively. Fluorescence is collected using the same microscope objective, and recorded with a spectrometer consisted of a 50 cm monochromator and a CCD camera (spectral resolution: 0.15 nm around 590 nm) using an exposure time of 0.5 s. A readout time of 1.6 s follows each exposure of the CCD camera. A shutter is used to unblock the green laser only during the exposure times of the CCD camera, while a shutter is not used in the infrared laser beam path; individual microdroplets are continuously excited by the infrared laser at varying powers during the experiments.

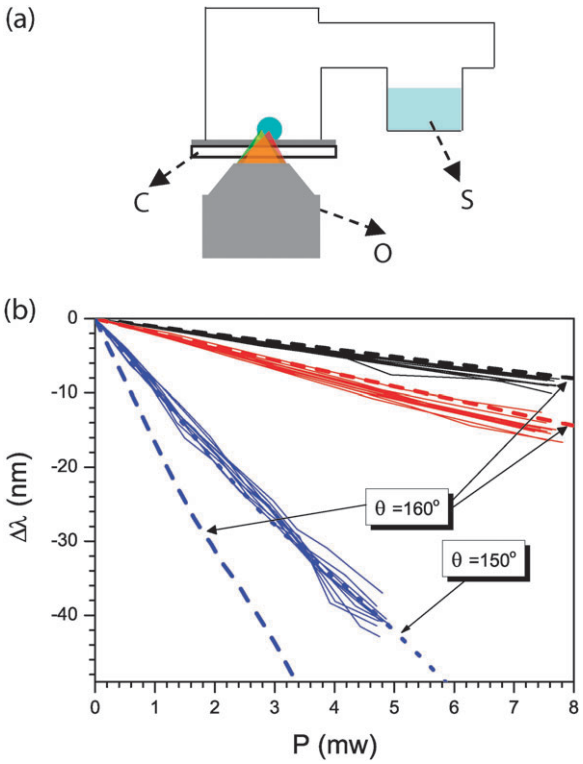

Fig. 1 (a) Illustration of the humidity chamber used in the experiments. S: saturated salt–water solution, C: superhydrophobically coated cover glass, and O: microscope objective. (b) Sensitivity of experimental (solid lines) and computational (dashed and dotted lines) spectral drifts as a function of infrared laser power for $S_A = 0.753$ (black), 0.8434 (red), and 0.973 (blue). Diameters of the microdroplets used in the experiments range between 7–11 μm. Computations are performed for a 7 μm diameter microdroplet considering contact angles of $\theta = 160°$ (dashed lines) and $\theta = 150°$ (dotted line).

Spectral drifts measured as a function of the incident laser power are plotted in Fig. 1b for three relative water humidities together with the computational results. Measurements shown in Fig. 1b are performed using microdroplets with diameters ranging between 8.2–10.0 μm, 8.3–10.0 μm, and 7.1–10.6 μm for S_A values of 0.753, 0.8434, and 0.973, respectively. This Figure shows that the spectral drifts are essentially independent of the microdroplet size, which is consistent with the results obtained for the glycerol–water system reported in ref. 5. Fig. 1b also indicates that the computational results are highly sensitive to the contact angle, especially for high humidity conditions. For instance, when the contact angle is considered to be 160° the spectral drifts are predicted very well for $S_A = 0.753$ and 0.8434 while there is significant discrepancy between the computational and experimental results for $S_A = 0.973$. However, for this relative humidity the computational results match very well with the experimental data when the contact angle is reduced to 150°. In fact, the measurements of quality factors of the WGMs support this deviation in the contact angle. Average quality factors of the WGMs are measured to be 1500 for $S_A = 0.973$, and almost

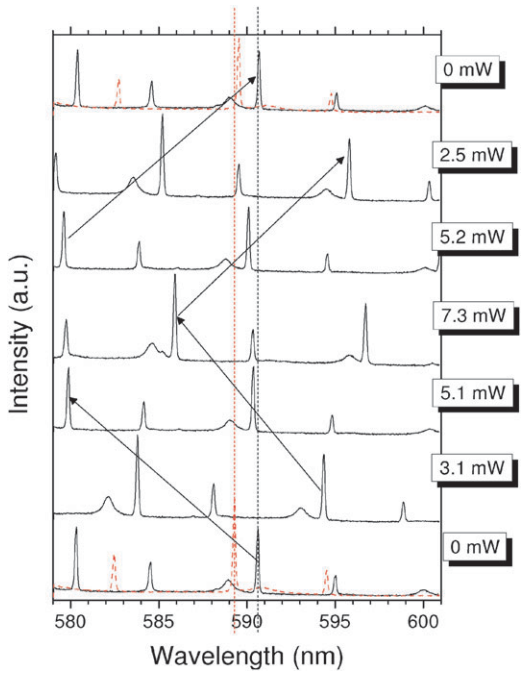

Fig. 2 Solid curves are the emission spectra recorded from a 8.3 μm diameter NaCl–water microdroplet as the infrared laser power is first increased from and then decreased to zero. Relative humidity in the experiment is S_A = 0.8434. Maximum spectral drift is 15.3 nm at an infrared laser power of 7.3 mW. Dashed curves are the emission spectra recorded at the beginning and end of the experiment from a 7.1 μm diameter reference microdroplet that is not exposed to the infrared laser. Arrows indicate the spectral drift of individual WGMs.

resolution limited at 3000 and 3300 for S_A = 0.753, and 0.8434, respectively. These results indicate that the average contact angle is higher at S_A = 0.753 and 0.8434 than that at S_A = 0.973. Approximations made in the lumped system model and error in the calculation of $\tilde{Q}_{abs}$ due to the presence of the substrate are other sources of errors in the computational results.

The main objective of the present study is to demonstrate full reversibility of the photothermal tuning mechanism. For this purpose, the fluorescence spectra are recorded as the incident laser power (P_{inc}) is first increased from zero to a maximum value and is then decreased back to zero. Fluorescence spectra from a second reference microdroplet are also recorded at the beginning and end of each hysteresis experiment in order to check for any fluctuations in the relative humidity in the chamber during the experiment. Such exemplary fluorescence spectra recorded from a photothermally tuned microdroplet and a reference microdroplet are shown in Fig. 2. Upon exposure to 7.3 mW infrared laser power, a maximum blue-shift of 15.3 nm is observed in the WGMs of the photothermally tuned microdroplet. At the end of the experiment when the infrared laser is completely blocked, the WGMs of the photothermally tuned and reference microdroplets are observed to be red-shifted with respect to their spectral positions at the beginning of the experiment by 0.06 nm and 0.26 nm, respectively. This implies a total reversibility of 1.3% in photothermal tuning. Spectral drifts observed in the WGMs of three microdroplets as P_{inc} is increased from and decreased back to zero are

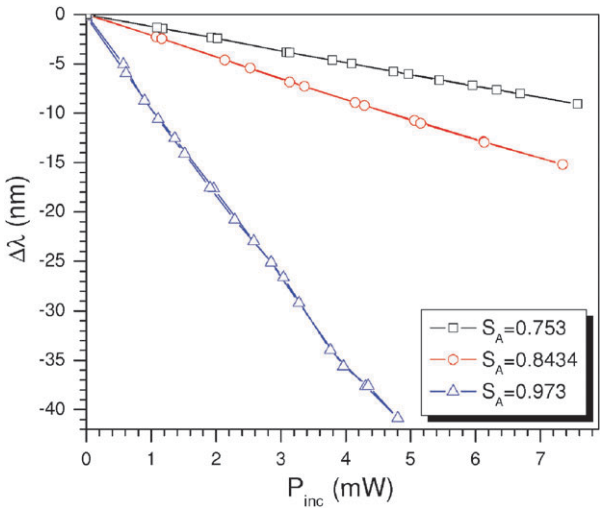

Fig. 3 Spectral drifts observed in three NaCl–water microdroplets as the infrared laser power is first increased from and decreased to zero, for three different relative humidities. Microdroplet diameters are 8.3, 8.3 and 7.7 μm for S_A = 0.753, 0.8434, and 0.973, respectively.

shown in Fig. 3. When the reference microdroplets are taken into account, the reversibilities observed for the microdroplets kept at S_A = 0.753, 0.8434, and 0.973 are calculated as 0%, 1.3%, and 0.6%, respectively. These values are within the experimental error range and they are much smaller than the irreversibilities observed in glycerol–water microdroplets.[5]

Yet another proof for the fully reversible photothermal tuning of NaCl–water microdroplets is demonstrated in Fig. 4 where consecutive fluorescence spectra recorded from a NaCl–water (Fig. 4a) and a glycerol–water (Fig. 4b) microdroplet kept at S_A = 0.8434 are shown. In these experiments, the total delay time between consecutive spectra is 7.1 s, including the exposure and readout times of the CCD camera, and a 5 s delay. For both the NaCl–water and glycerol–water microdroplets the infrared laser is completely blocked during the first 30 acquisitions. Almost constant spectral positions of the WGMs during these periods indicate the high stability of the relative humidity in the chamber. NaCl–water and glycerol–water microdroplets are then exposed to the infrared laser at powers of 4.6 mW and 4.4 mW, respectively. At acquisition 30, blue-shifts by 10.0 nm and 8.9 nm are observed in the WGMs of the NaCl–water and glycerol–water microdroplets, respectively. Following a slight blue-shift by 0.1 nm until the acquisition 35, the WGMs of the NaCl–water microdroplet remain stationary at their spectral positions between acquisitions 35 and 140. This indicates that no further evaporation is observed in the NaCl–water microdroplet while it is exposed to the infrared laser. In contrast, the WGMs of the glycerol–water microdroplet are observed to drift to blue wavelengths until acquisition 163 by 10.6 nm, at an almost constant rate. For the NaCl–water microdroplet when the infrared laser is blocked again at acquisition 140, a red-shift is observed in the WGMs, almost fully recovering their initial spectral positions before acquisition 30. Final stable spectral positions of the WGMs are observed to be red shifted by only 0.05 nm compared to their initial spectral positions. This demonstrates the full reversibility of the photothermal tuning

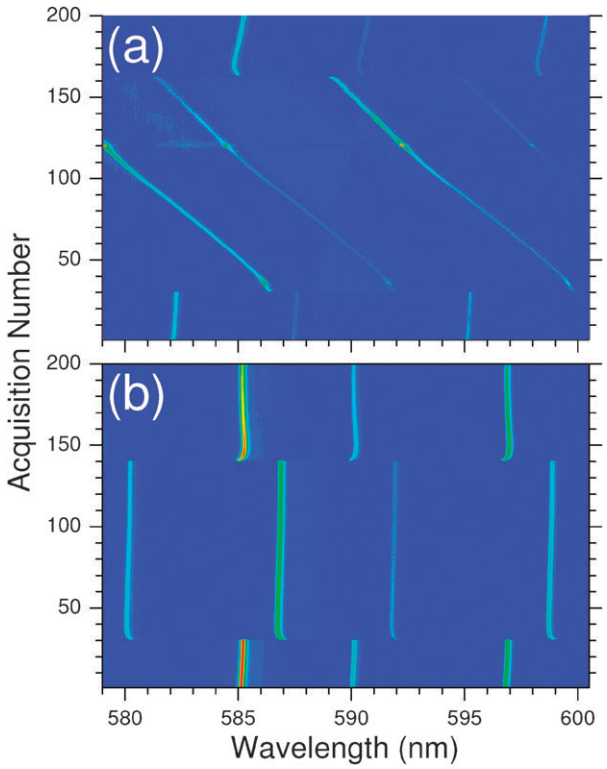

Fig. 4 Consecutive emission spectra recorded from a 6.5 μm diameter glycerol–water microdroplet (a) and a 7.7 μm diameter NaCl–water microdroplet (b). Intensity values in arbitrary units increase from blue to red. Microdroplets are exposed to infrared laser between acquisitions 30–163 and 30–140 in (a) and (b), respectively. Infrared laser power is 4.6 mW and 4.4 mW in (a) and (b).

of the NaCl–water microdroplet. In contrast, for the glycerol–water microdroplet, after the laser is blocked at acquisition 163 the WGMs are observed to be blue-shifted by almost 10 nm with respect to their initial spectral positions before acquisition 30.

In conclusion, fully reversible spectral tuning of NaCl–water microdroplets standing on a superhydrophobic surface using local heating by a focused infrared laser has been demonstrated. Experiments revealed reversible photothermal tuning by up to $\sim$40 nm, with no fundamental limitations on increasing the tuning range. A good agreement is reached between the experimental results and computations performed using a model that considers a lumped system formulation of mass and energy conservations. The presented technique may find applications in short-haul optical communication systems, water-based opto-fluidics systems, and fundamental studies in aerosol chemistry. It may also be used in super-hydrophobic surface characterization, especially because of the high sensitivity of the spectral tuning to the contact angle.

Acknowledgements

The authors thank the Alexander von Humboldt Foundation for equipment donation. A. Kiraz acknowledges the financial support of the Turkish Academy of Sciences in the framework of the Young Scientist Award program (Grant No. A.K/TÜBA-GEBIP/2006-19).

References

1 J. P. Reid, H. Meresman, L. Mitchem and R. Symes, *Int. Rev. Phys. Chem.*, 2007, **26**, 139–192.
2 K. J. Vahala, *Nature*, 2003, **424**, 839.
3 M. M. Dumitrescu, M. J. Saarinen, M. D. Guina and M. V. Pessa, *IEEE J. Quantum Electron.*, 2002, **8**, 219–230.
4 D. Psaltis, S. R. Quake and C. Yang, *Nature*, 2006, **442**, 381–386.
5 A. Kiraz, Y. Karadağ and M. Muradoğlu, *Phys. Chem. Chem. Phys.*, 2008, **10**, 6446–6454.
6 A. J. Campillo, C. J. Dodge and H.-B. Lin, *Appl. Opt.*, 1981, **20**, 3100–3103.
7 S. Arnold and A. B. Pluchino, *Appl. Opt.*, 1982, **21**, 4194–4196.
8 S. Arnold, M. Neuman and A. B. Pluchino, *Opt. Lett.*, 1984, **9**, 4–6.
9 S. Arnold, E. K. Murphy and G. Sageev, *Appl. Opt.*, 1985, **24**, 1048–1053.
10 H. Tu and A. K. Ray, *Chem. Eng. Commun.*, 2005, **192**, 474–498.
11 R. G. Picknett and R. J. Bexon, *J. Colloid Interface Sci.*, 1977, **79**, 667–677.
12 G. McHale, S. Aqil, N. J. Shirtcliffe, M. I. Newton and H. Y. Erbil, *Langmuir*, 2005, **21**, 11053–11060.
13 I. N. Tang, A. C. Tridico and K. H. Fung, *J. Geophys. Res., [Atmos.]*, 1997, **102**, 23269–23275.
14 G. Grehan, B. Maheu and G. Gouesbet, *Appl. Opt.*, 1986, **25**, 3539–3548.
15 J. A. Lock, *Appl. Opt.*, 1995, **34**, 559–570.
16 J. A. Lock, *J. Opt. Soc. Am. A*, 1998, **15**, 2986–2994.
17 E. J. G. Peterman, F. Gittes and C. F. Schmidt, *Biophys. J.*, 2003, **84**, 1308–1316.
18 J. Lin and C. W. Brown, *Appl. Spectrosc.*, 1993, **47**, 239–241.

